

Alteration sequence of CV3 chondrites: matrix textures and Raman spectroscopy. M. Komatsu^{1,2}, T. J. Fagan², T. Mikouchi³, and A. Yamaguchi⁴, ¹The Graduate University for Advanced Studies (komatsu_mutsumi@soken.ac.jp), ²Department of Earth Sciences, Waseda University, ³Department of Earth and Planetary Science, University of Tokyo, ⁴National Institute of Polar Research.

Introduction:

The CV chondrites form a diverse group of meteorites divided into three subgroups: oxidized Bali-like (CV_{oxB}); oxidized Allende-like (CV_{oxA}); and reduced CV (CV_{red}) chondrites. It has been suggested that the main differences in mineral assemblages and textures between the CV subgroups were caused by variable conditions of alteration/metamorphism (e.g., [1]). The CV_{oxB} subgroup (e.g., Kaba, Bali) experienced hydrous alteration [2], but apparently escaped a subsequent episode of strong thermal metamorphism. On the other hand, the CV_{oxA} subgroup (e.g., Allende, ALH 84128) experienced thermal metamorphism. The reduced CV chondrites (e.g., Efremovka, Leoville) experienced metamorphism similar to that of CV_{oxA}, but of a smaller degree [3].

In this study, we examine a set of type 3 carbonaceous chondrites in order to examine how the secondary characteristics in matrix and the structural grade of organic matter can be used as indicators of alteration processes of CV chondrites.

Methods:

Eight CV chondrites and one CO chondrite are examined in this study (Table 1). Some of the assigned subtypes are tentative, as they are based mostly on the petrography of amoeboid olivine aggregates (AOAs; to be presented in [4]). Because all CV chondrites in this study have undergone varying degrees and types of alteration, we compare these samples with CO chondrite Y-81020 (CO3.05), which is one of the most primitive carbonaceous chondrites [e.g., 5]. The petrographic study was performed using a Hitachi S-4500 SEM at University of Tokyo, and JEOL JXA-8900 EPMA at Waseda University. Raman spectra were collected using a JASCO Raman Spectrometer at National Institute of Polar Research. Analytical parameters are similar to those in [6].

Results and Discussion:

Raman Spectra Analysis

Raman spectroscopy is very sensitive to the degree of structural order of polyaromatic organic matter (OM). The typical Raman spectrum of such a material exhibits several bands, including G-band (~1600cm⁻¹, from graphite) and D-band (~1350cm⁻¹, from defects). It has been suggested that FWHM-D (full width at half maximum of the D-band) decreases with increasing maturity of OM, and I_D/I_G (ratio of intensities of the D- and G-bands) is sensitive to heating conditions [7]. As metamorphic subtype increases, Raman FWHM-D decreases and

I_D/I_G increases in ordinary chondrites [7], and the same is apparently true of CV chondrites [6].

In previous studies [e.g., 6], Raman spectra were collected from the meteorite raw samples. Instead, we collected Raman spectra from polished thin sections (PTS). The Raman tracers (FWHM-D vs. I_D/I_G) obtained from PTS from Efremovka and Allende show similar values to those collected from raw samples by [6], suggesting reliable OM maturity can be also obtained from PTS.

Of seven chondrites in this study, six chondrites exhibit D- and G-bands. Raman spectra from Y-86751 showed only weak D- and G-bands so the decomposition of spectra was not successful. Y-86751 PTS has evidence of terrestrial weathering (oxidation of opaques), so Raman tracers may have been destroyed by terrestrial weathering.

Raman spectra from the CV chondrites Y-980145, Y-980145, A-881317, A-881837, and Y-86009 all have FWHM-D ~170-250 cm⁻¹ and I_D/I_G<1.1 (Fig. 1). These characteristics are similar to petrologic subtype 3.1-3.4 [6]. Among these CV chondrites, Y-980145 combines relatively high FWHM-D with small I_D/I_G ratio (Fig.1), suggesting low metamorphic subtype (PT≤3.1). In contrast, Allende has low FWHM-D and high I_D/I_G (Fig. 1) consistent with the high subtype (>3.6) assigned by [6].

Matrix petrography

If we accept the petrologic subtypes based on PTS Raman spectroscopy, it seems that matrix olivine grains show a general correlation between grain size and metamorphic subtype. In Y-81020, matrix olivine grains are generally so small (<0.5 μm) and grains are so closely compacted with adjacent grains that individual crystals are difficult to distinguish (Fig. 2a). Y-980145 and Efremovka also have fine-grained matrices (Fig. 2b,c). In comparison, the matrices of A-880835 and A-881317 appear to have slightly higher porosities and grain sizes (<1 μm; Fig. 2e,f). Olivine crystals in the matrix of Y-86009 tend to have lath-like shapes (< 1 to 5 μm) with pores between the laths (Fig. 2g). Zoning from Mg-rich cores to Fe-rich rims can be detected in some relatively large grains (Fig. 2g). Lath-like olivine is also characteristic of Kaba (<2 to 7 μm), but the olivine laths are coarser and pore spaces between them are wider than in Y-86009 (Fig. 2g,h). Two textural varieties of matrix were identified in Y-86751; matrix type Y-86751(B) is relatively fine-grained, whereas Y-86751(A) has coarser grains and is more porous (compare Figs. 2d and 2i). Y-86751(B) matrix shows incipient development of

porosity and appears to be intermediate between the very fine-grained group (Y-81020, Y-980145, Efremovka) and chondrites with obvious porosity. The most coarse-grained olivine laths (2 to 20 μm) and the widest, most continuous pore spaces (<2 μm) occur in Allende matrix (Fig. 2j).

Discussion:

The matrix textures can be classified into six groups from finest grain size and least porosity to coarser lath-like olivine and greater interconnected porosity as follows: (1) Y-81020, Y-980145, Efremovka; (2) Y-86751(B); (3) A-880835, A-881317, Y-86009; (4) Kaba; (5) Y-86751(B); (6) Allende. This classification does not imply that all of these meteorites are part of a common metamorphic progression. We note, however, that meteorites for which subtypes have been determined show some parallels with the matrix textures. Y-81020 is in the least porous group and is classified as a petrologic subtype (PT) 3.05, whereas Kaba, with fine lath-like olivine, is classified as a PT3.1, and Allende, with coarse olivine laths, is classified as PT>3.6 (Table 1). Efremovka is classified in a range from PT3.1 to 3.4 [6], but its non-porous texture does not appear to be intermediate in development of lath-like olivine between Kaba and Allende; however, matrix grains in Efremovka have been deformed by shock [8], which likely caused a reduction in porosity (e.g., [9]).

Although more work is needed to define the relationships between the matrix and the degree of secondary alteration, a general correlation between matrix grain size and maturity of OM is observed. It is consistent with our examination from chemical compositions of amoeboid olivine aggregates and matrix petrography of host meteorites [4]. It should be noted that the matrix grain sizes are also affected by shock compaction [8,9], and low-temperature aqueous alteration (e.g., [10]), thermal metamorphism and dehydration (e.g., [11]) may have played different roles for formation of matrix olivine.

References:

[1] Krot A. N. et al. (1998) *Meteorit. Planet. Sci.*, 33, 1065–1085. [2] Keller L. et al. (1994) *Geochim. Cosmochim. Acta*, 58, 5589–5598. [3] Weisberg M. K. and Prinz M. (1998) *Meteorit. Planet. Sci.*, 33, 1087–1099. [4] Komatsu et al., 2015 *Meteorit. Planet. Sci.*, accepted pending revision. [5] Grossman J.N. and Rubin A. E. (2006) 37th Lunar Planet. Sci. Conf. abstract #1383. [6] Bonal L. et al. (2006) *Geochim. Cosmochim. Acta*, 70, 1849–1863. [7] Quirico et al. (2003) *Meteorit. Planet. Sci.*, 38, 795–881. [8] Scott E. R. D. et al. (1992) *Geochim. Cosmochim. Acta*, 56:4281–4293. [9] MacPherson and Krot A. N. (2014) *Meteorit. Planet. Sci.*, 49, 1250–1270. [10] Krot A. N. et al. (2004) *Antarct. Meteorit. Research*, 17:153–171. [11] Cuvillier P. et al. (2014) 45th Lunar Planet. Sci. Conf. abstract #1708.

Name	Type	Subgroup	Dominant grain size of matrix olivine	Proposed PT ^a
Efremovka	CV	Reduced	<0.5 μm	3.1–3.4
Y-980145	CV	-	<0.5 μm	3.1 ^c
Y-86009	CV	Oxidized Bali ^b	<1.5 μm	3.1–3.4 ^c
Kaba	CV	Oxidized Bali	<2.7 μm	~3.1
A-881317	CV	-	<2.7 μm	3.1–3.4 ^c
A-880835	CV	-	<2.7 μm	3.1–3.4 ^c
Y-86751	CV	Oxidized Bali/Allende ^b	<1 μm (lith. B) <2 to 10 μm (lith. A)	not available
Allende	CV	Oxidized Allende	2–20 μm	>3.6
Y-81020	CO	-	<0.5 μm	3.05

^aPetrologic types proposed by Bonal et al. (2006) for CV chondrites, and Grossman and Rubin (2006) for Y-81020.

^bTentative subgroup classifications for Y-980145, Y-86009, and Y-86751 based on the petrography of AOA's described in Komatsu et al. (2015).

^cTentative petrologic types for Y-980145, Y-86009, A-881317, and A-880835 based on Raman spectra in this study.

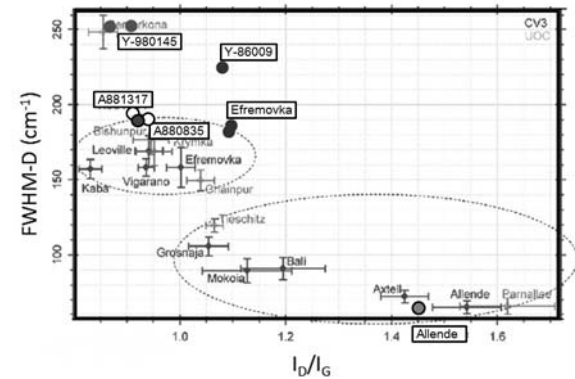


Fig.1. Spectral parameters of Raman bands of carbonaceous materials in CV chondrites in this study plotted on Bonal et al. (2006) [6].

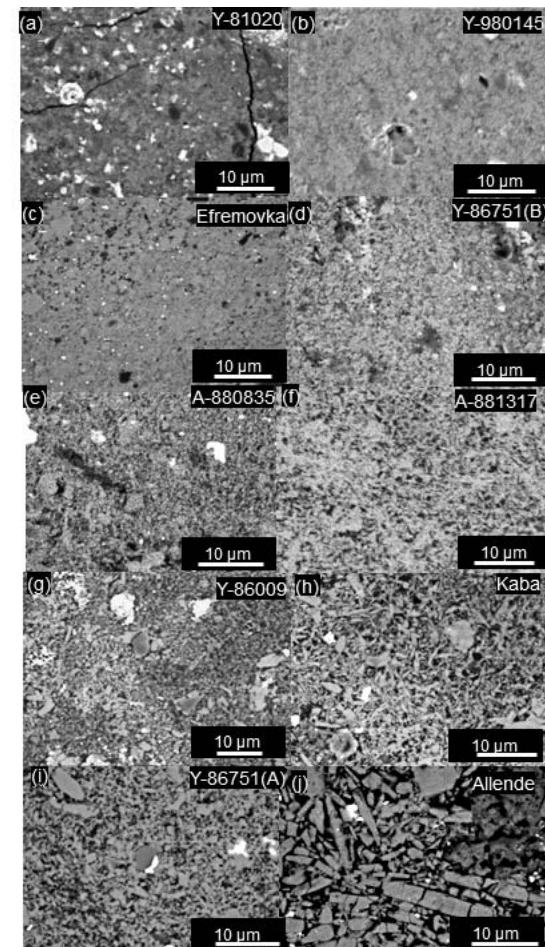


Fig.2. BSE images of matrices of chondrites.